Dinuclear Reductive Eliminations

Georges Trinquier and Roald Hoffmann*

Department of Chemistry, Cornell University, Ithaca, New York 14853

Received July 21, 1983

Intramolecular dinuclear 1,2-reductive elimination reactions are not common in organotransition-metal chemistry, and this paper describes why this is so. Qualitative molecular orbital theory is used to study the model reaction: $L_4(H)M—M(H)L_4 \rightarrow H_2 + L_4M{=}ML_4$. This reaction is symmetry forbidden and exhibits a large activation energy for a C_{2v} concerted least-motion pathway, like its organic analogue, cis elimination of H_2 from ethane. The energy barrier is reduced considerably for a pathway that starts with a cis bending of the M–H bonds, bringing the hydrogen atoms together, and forming first the H–H bond. Lower symmetry, nonconcerted pathways and substituents may be used to lower the activation energy for the reaction a bit further, but the reaction remains fundamentally an unfavorable one.

Reductive eliminations and their microscopic reverse reactions, oxidative additions, are an important class of reactions in organotransition-metal chemistry.[1] Most of them occur from mononuclear complexes (**1**). Some may involve two molecules (dinuclear bimolecular reactions), but similar reactions occurring intramolecularly in a dinuclear complex containing a metal–metal bond, the order of which is changed (**2**), appear to be virtually nonexistent.

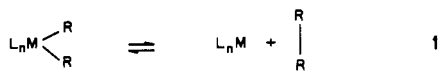

1

2

Let us review some known reactions that might be related to some extent to the reaction shown in **2**. Chisholm et al.[2] have reported a puzzling reaction (**3**) that involves both CO_2 insertion and reductive elimination from a group 6 dinuclear complex. Labeling experiments have shown that this reaction is stepwise, the reductive elimination occurring via a β-hydrogen elimination on one metal center.

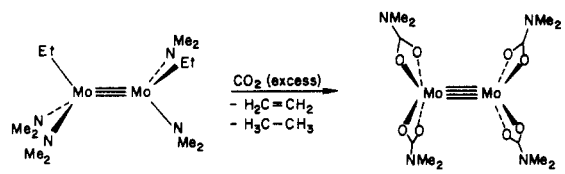

d^3 d^4

3

The same group has reported oxidative additions of peroxides and halogens to dimolybdenum(III) complexes.[2c,d] Addition of peroxides, as shown in **4**, gives a bridged compound containing a formally double metal–metal bond. It has been suggested that the dialkyl peroxide first coordinates to the dimetal center before O–O bond cleavage and oxidative addition is achieved. However, due to the weakness of the O–O bond in peroxides, a multiple-step

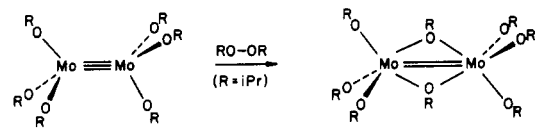

d^3 d^2

4

mechanism, first involving the breaking of this O–O bond, must not be excluded.

Reaction with halogens generally involves the addition of two molecules of X_2 (**5**), giving a bridged complex con-

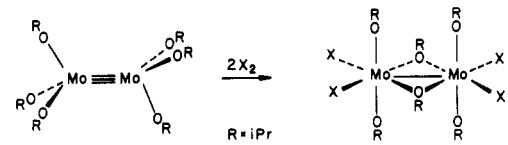

d^3 d^1

5

taining a metal–metal single bond. In this case, it is difficult to imagine a concerted dinuclear addition. The product obtained would suggest two mononuclear additions on each metal center, but it is rather presumed that the reaction begins by the addition to one molecule of X_2 to give the intermediate $Mo_2(OR)_6X_2$ that is unstable toward disproportionation to $Mo_2(OR)_6$ and $Mo_2(OR)_6X_4$.

Norton et al.[3,4] have found that the easy reductive elimination of alkane from alkyl hydride complexes of osmium is dinuclear and intermolecular (**6**). The product,

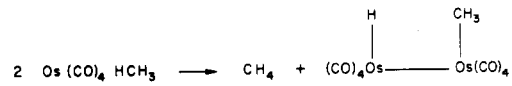

6

which is a d^7 18-electron compound, does not provide a further intramolecular reductive elimination of alkane. The mechanism of reaction **6** has been further investigated kinetically; the symmetrical dihydride or dialkyl compounds, which are more common, undergo far less easily this reductive elimination, which is characteristic of the

(1) See for instance: Collman, J. P.; Hegedus, L. S. "Principles and Applications of Organotransition Metal Chemistry"; University Science Books: Mill Valley, CA 1980; p 176.

(2) (a) Chisholm, M. H.; Haitko, D. A.; Murillo, C. A. *J. Am. Chem. Soc.* **1978**, *100*, 6262. (b) Chisholm, M. H.; Haitko, D. A. *Ibid.* **1979**, *101*, 6784. (c) Chisholm, M. H., to be submitted for publication. (d) Chisholm, M. H.; Kirkpatrick, C. C.; Huffman, J. C. *Inorg. Chem.* **1981**, *20*, 871.

(3) Okrasinski, S. J.; Norton, J. R. *J. Am. Chem. Soc.* **1977**, *99*, 295.

(4) Norton, J. R.; Carter, W. J.; Keeland, J. W.; Okrasinski, S. J. In "Transition Metal Hydrides"; Bau, R., Ed.; American Chemical Society: Washington, DC, 1978; p 170.

0276-7333/84/2303-0370$01.50/0

Scheme I

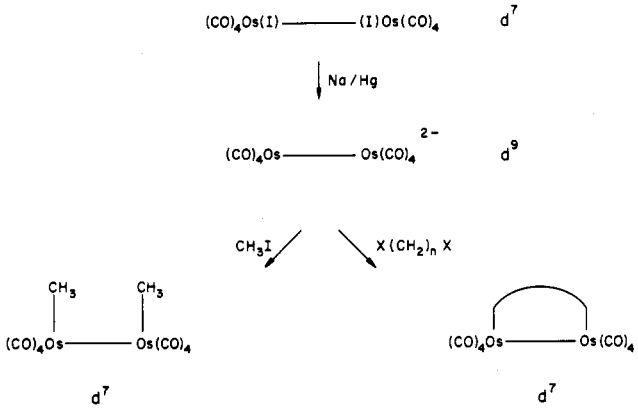

mixed alkyl hydrido complex.

The sequence of reactions (Scheme I), observed on a dinuclear complex of osmium, shows a reductive elimination followed by oxidative additions, yielding 1,2-dimethyl or dimetallacycloalkyl complexes.[5a] The dimethyl compound can eliminate a methane to give a methylene-bridged compound that in turn can add an ethylene molecule to give a dimetallacyclopentane product, but those reactions do not change the oxidation state of the metal.

The dimetallacyclobutane product **7** is another example

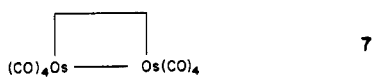

7

of a d^7 18-electron dinuclear complex that is relatively stable with respect to 1,2-reductive elimination (of ethylene in this case). In fact one of the modes of formation of **7** is by a photochemical reaction from $Os_3(CO)_{12}$ involving a possible $Os_2(CO)_8$ intermediate.[5b] The diosmacyclobutane **7** does eliminate ethylene cleanly at 100 °C.[5c]

Trans oxidative additions of halogens on d^8 16-electron square-planar dinuclear complexes of rhodium have been reported. In these reactions, such as **8a** and **8b**, an 18-electron complex is formed while the bond order between the metals is promoted from 0 to 1.[6]

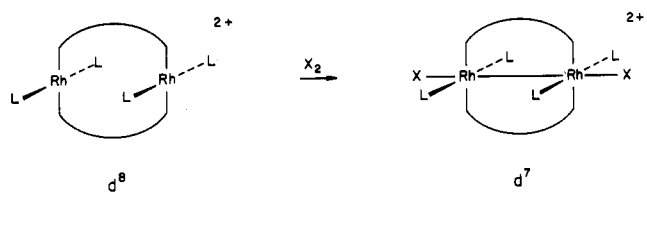

L = RNC
Bridging ligands = $(Ph_2P)_2CH_2$
X = Cl, Br, I

8a

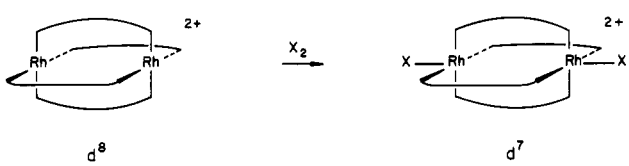

Bridging ligand = $CN(CH_2)_3NC$
X = Cl, Br, I

8b

(5) (a) Motyl, K. M.; Norton, J. R.; Schauer, C. K.; Anderson, O. P. *J. Am. Chem. Soc.* **1982**, *104*, 7325. (b) Burke, M. R.; Takats, J.; Grevels, F.-W.; Reuvers, J. G. A. *Ibid.* **1983**, *105*, 4092. For other dimetallacyclobutanes see also: ref 9c and Green, M.; Laguna, A.; Spencer, J. L.; Stone, F. G. A. *J. Chem. Soc., Dalton Trans.* **1977**, 1010. (c) Norton, J. R., private communication.

Scheme II

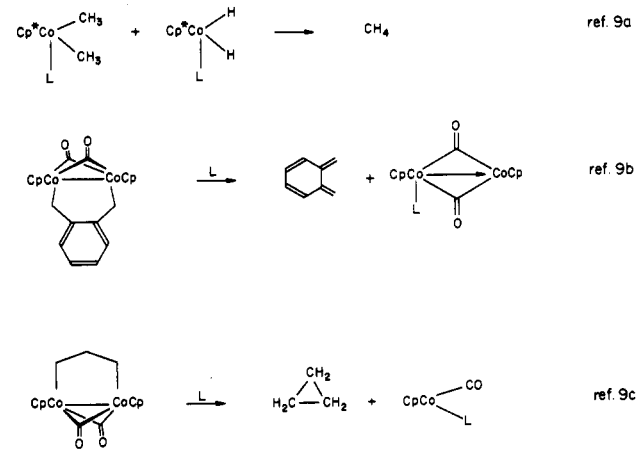

Brown, Fisher, Hill, Puddephatt, and Seddon[7] have reported a dinuclear reductive elimination of H_2 from a d^8 platinum(II) complex (**9**). The mechanism may or may

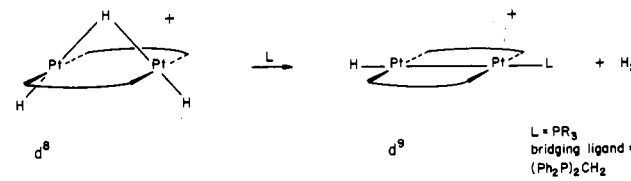

9

not involve the elimination of H_2 at a single metal center. Two-center oxidative additions on pyrazolyldiiridium(I) complexes have been studied by Stobart et al.[8] (**10**). In some cases (addition of I_2, MeI) one can see that formation of an iridium–iridium bond does not occur since the corresponding intermetallic distance remains long.

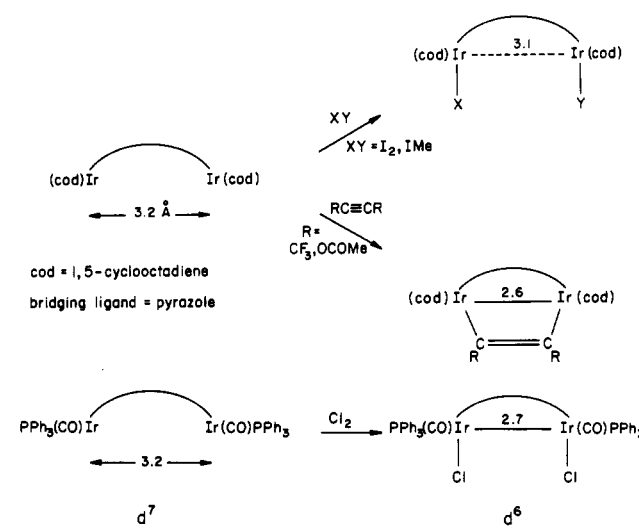

10

(6) Felthouse, T. R. *Prog. Inorg. Chem.* **1982**, *29*, 73.

(7) Brown, M. P.; Fisher, J. R.; Hill, R. H.; Puddephatt, R. J.; Seddon, K. R. *Inorg. Chem.* **1981**, *20*, 3516. Hill, R. S.; Puddephatt, R. J. *J. Am. Chem. Soc.* **1983**, *105*, 5797.

(8) (a) Coleman, A. W.; Eadie, D. T.; Stobart, S. R.; Zaworotko, M. J.; Atwood, J. L. *J. Am. Chem. Soc.* **1982**, *104*, 922. (b) Beveridge, K. A.; Bushnell, G. W.; Dixon, K. R.; Eadie, D. T.; Stobart, S. R.; Atwood, J. L.; Zaworotko, M. J. *Ibid.* **1982**, *104*, 920. (c) Bushnell, G. W.; Fjeldsted, D. O. K.; Stobart, S. R.; Zaworotko, M. J. *J. Chem. Soc., Chem. Commun.* **1983**, 580.

Bergman, Janowicz, Hersh, and Theopold[9] have discovered several reactions that could be dinuclear eliminations (Scheme II), but the mechanism of these fascinating processes is not yet known.

These are some reactions that can be related to dinuclear reductive eliminations or oxidative additions. Other examples can be found in the literature.[10] It appears that none of these reactions is a proven simple clear-cut concerted 1,2-reductive elimination (or oxidative addition) from a dinuclear complex.[10m] It seems therefore that the intramolecular reductive elimination from a dinuclear compound is not an easy reaction.

There have been some theoretical studies on mononuclear reductive elimination reactions,[11] including recent ab initio calculations on reductive elimination from NiR_2.[12] The purpose of the present work is to analyze theoretically intramolecular dinuclear reductive elimination reactions such as **2**. To this end, we shall use one-electron arguments supported by extended Hückel calculations. Several simplifications and assumptions will be made all along this work. The leaving group R_2 in **2** will be H_2, and idealized geometries with high symmetry will be used. The details concerning geometries, reaction coordinates, and extended Hückel parameters are given in the Appendix.

The Least-Motion C_{2v} Pathway. A reasonable model system for the prototype concerted dinuclear elimination is **11** → **12**, $L_4Mn(H)$–$Mn(H)L_4^{2-}$. We began our calculations with L = CO but then moved to a simpler model with L = H^-. The hydride model preserved the essential features of the reaction path.

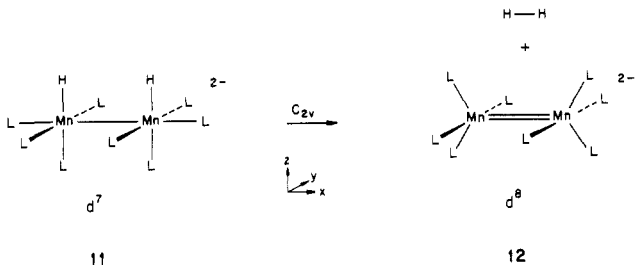

11 **12**

Since the extended Hückel method cannot be used reliably for a complete potential energy surface when bond lengths change drastically, we chose a hypothetical C_{2v} reaction path between reactants and products. The details of the path are given in the Appendix. Here we mention that it connects an octahedral **11**, Mn—Mn = 2.90 Å, with a model **12**, Mn=Mn = 2.40 Å and H—H = 0.74 Å, local coordination geometry trigonal bipyramidal at each metal. The final point of the reaction is assumed to occur when the centers of the M–M and H–H bonds are separated by 4 Å. The reaction coordinate, which we emphasize again is assumed, consists of 10 synchronous regular variations of bond lengths, bond angles, and dihedral angles connecting reactant **11** with product **12**, while maintaining C_{2v} symmetry.

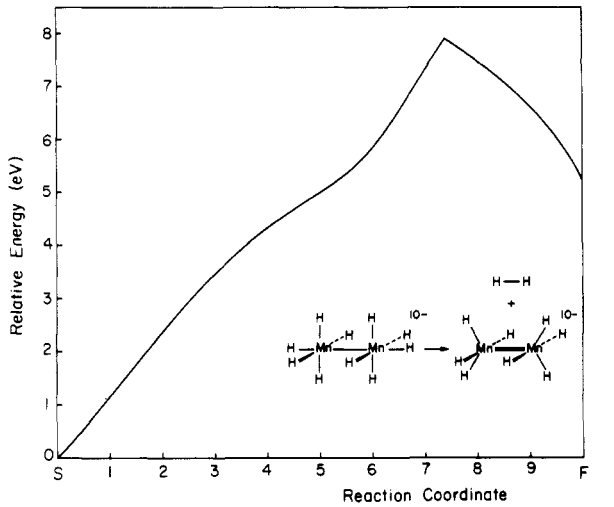

Figure 1. Variation of total energy along the C_{2v} least-motion reductive elimination of H_2 from $Mn_2H_{10}^{10-}$.

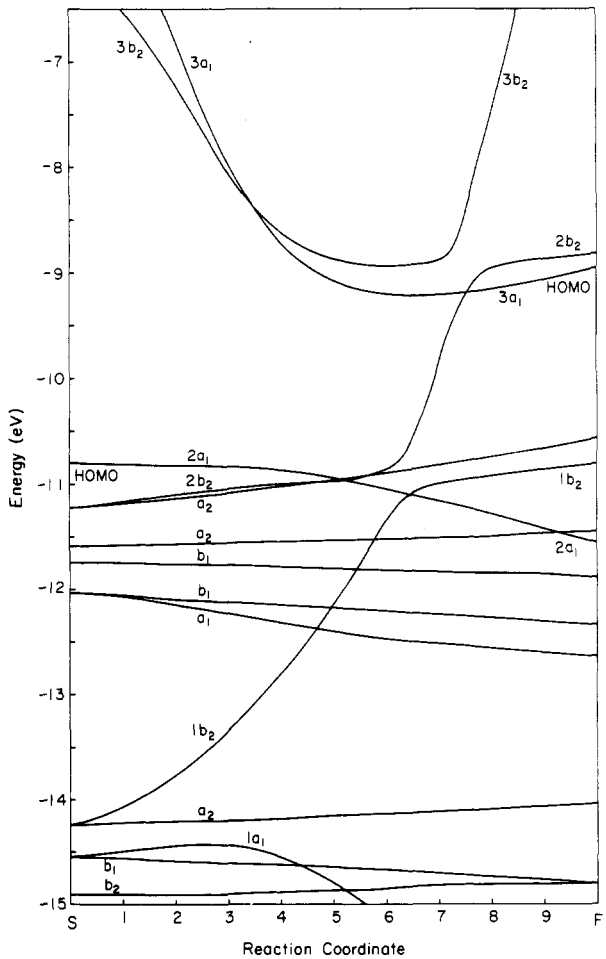

Figure 2. Orbital correlation diagram for the C_{2v} least-motion reductive elimination of H_2 from $Mn_2H_{10}^{10-}$.

(9) (a) Janowicz, A.; Bergman, R. G. *J. Am. Chem. Soc.* **1981**, *103*, 2488. (b) Hersh, W. H.; Bergman, R. G. *Ibid.* **1981**, *103*, 6992. (c) Theopold, K. H.; Bergman, R. G. *Ibid.* **1980**, *102*, 5695; **1981**, *103*, 2489; *Organometallics*, **1982**, *1*, 219; **1982**, *1*, 1571.

(10) (a) Davidson, P. J.; Lappert, M. F.; Pearce, R. *Chem. Rev.* **1976**, *2*, 219. (b) Schrock, R. R.; Parshall, G. W. *Ibid.* **1976**, *2*, 243. (c) Chisholm, M. H.; Rothwell, I. P. *Prog. Inorg. Chem.* **1982**, *29*, 1. (d) Cotton, F. A. *Chem. Soc. Rev.* **1983**, *12*, 35. (e) Manojlović-Muir, L.; Muir, K. W. *J. Chem. Soc., Chem. Commun.* **1982**, 1155. (f) Puddephatt, R. J.; Thomson, M. A.; Manojlović-Muir, L.; Muir, K. W.; Frew, A. A. *Ibid.* **1981**, 805. (g) Frew, A. A.; Hill, R. H.; Manojlović-Muir, L.; Muir, K. W.; Puddephatt, R. J. *Ibid.* **1982**, 198. (h) Pringle, P. G.; Shaw, B. L. *Ibid.* **1982**, 81. (i) Chisholm, M. H.; Huffman, J. C.; Kirkpatrick, C. C. *Inorg. Chem.* **1983**, *22*, 1704. (j) Arnold, D. P.; Bennet, M. A.; McLaughlin, G. M.; Robertson, G. B.; Whittaker, M. J. *J. Chem. Soc., Chem. Commun.* **1983**, 32. (k) Arnold, D. P.; Bennet, M. A.; McLaughlin, G. M.; Robertson, G. B. *Ibid.* **1983**, 34. (l) Norton, J. R., private communication. (m) A recent example that may be such a direct elimination is the evolution of H_2 from $[CpFeH(CO)]_2[Ph_2PCH_2CH_2PPh_2]$ at 90 °C: Davies, S. G.; Hibberd, J.; Simpson, S. J.; Watts, O. *J. Organomet. Chem.* **1982**, *238*, C7. (n) Bitterwolf, T. E. *J. Organomet. Chem.* **1983**, *252*, 305.

(11) (a) Komiya, S.; Albright, T. A.; Hoffmann, R.; Kochi, J. K. *J. Am. Chem. Soc.* **1976**, *98*, 7255. (b) Tatsumi, K.; Hoffmann, R.; Yamamoto, A.; Stille, K. *Bull. Chem. Soc. Jpn.* **1981**, *54*, 1857. (c) Hoffmann, R. In "IUPAC Frontiers of Chemistry"; Laidler, K. J., Ed.; Pergamon Press: Oxford, 1982; p 247.

(12) (a) Blomberg, M. R. A.; Siegbahn, P. E. M. *J. Chem. Phys.* **1983**, *78*, 5682. (b) Blomberg, M. R. A.; Siegbahn, P. E. M., submitted for publication.

The energy profile so calculated for **11** → **12**, L = H^-, is shown in Figure 1. The corresponding orbital correlation diagram is displayed in Figure 2. A clear level crossing occurs between b_2 and a_1 molecular orbitals (MO) that are respectively occupied and unoccupied in the starting product. The reaction is therefore forbidden under this symmetry, and actually a barrier of 7.9 eV occurs while the reaction energy is 5.2 eV in favor of the oxidized reactant.

Let us analyze the electronic structure of reactant and product to see how this level crossing comes about. The metal–metal single bonded $M_2H_{10}^{10-}$ can be constructed simply from the interaction of two d^7 ML_5 fragments. The orbitals of these fragments are well-known,[13] consisting of a directed hybrid, a_1, above three "t_{2g}" levels (**13**). Two

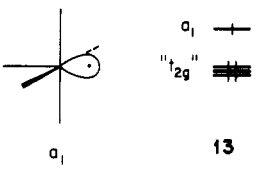

13

such fragments combine to give a σ and σ^* pair, as shown schematically in **14**. This simple picture may be perturbed

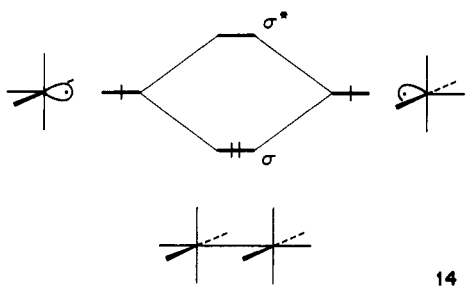

14

by further orbital mixing but actually is fairly well preserved in the actual calculation of $Mn_2H_{10}^{10-}$. The metal–metal σ bond is $2a_1$, and the band of six levels directly below it comprises the t_{2g} levels of two metals, weakly interacting with each other.

The final product d^8 M_2L_8 is unsaturated and bears a formal metal–metal double bond. We have chosen for our models a nonbridged D_{2h} geometry, but we are conscious that this may not necessarily be the preferred form for such a species which may happen to be kinetically unstable, as $Fe_2(CO)_8$ is. The bonding in the product again can be analyzed in terms of two interacting d^8 ML_4 fragments. A d^8 C_{2v} ML_4 fragment is isolobal with CH_2, i.e., has two orbitals b_2 and a_1 occupied by two electrons and ready for double bonding (**15**). The ordering of the two orbitals a_1

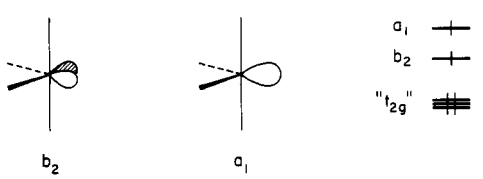

15

and b_2 differs for CH_2 and ML_4, but this is not important for the construction of their dimers. The scheme of bonding in $Mn_2H_8^{10-}$ is given in Figure 3. That diagram is typical of a doubly bonded highly unsaturated species.

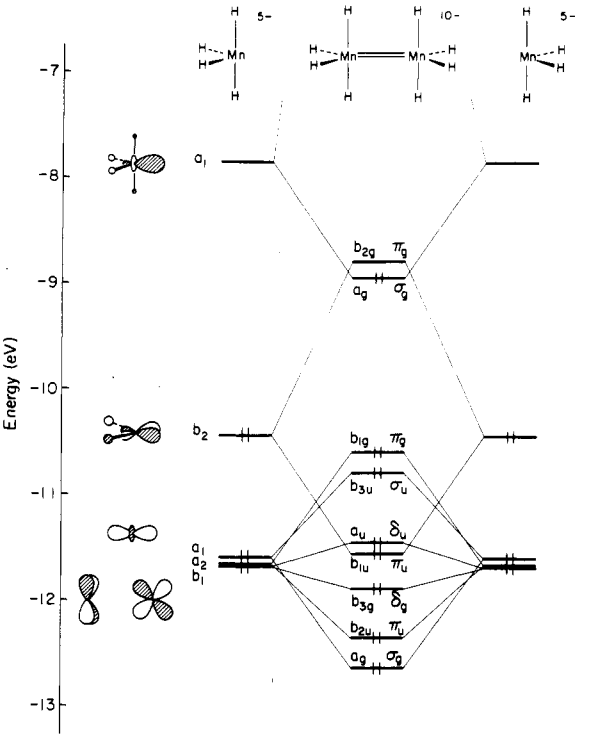

Figure 3. Interaction diagram of the two MnH_4^{5-} fragments in $Mn_2H_8^{10-}$.

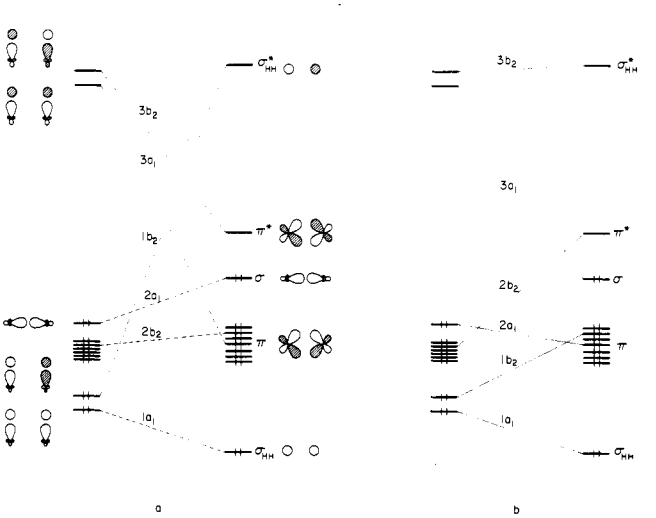

Figure 4. Schematic correlation diagrams for the elimination of H_2 from a d^7 transition-metal complex $L_4(H)M–M(H)L_4$: (a) before taking into account the avoided level crossings; (b) after taking into account the avoided level crossings.

The two occupied MO's that are responsible for the bonding are b_{1u} (d_π) and the HOMO a_g (d_σ). The LUMO, b_{2g}, has d_{π^*} character. The very small HOMO–LUMO gap shows the extremely unsaturated, and therefore reactive, character of this model molecule.

Let us see now in detail what happens in Figure 2 during the reaction **11** → **12**. As soon as the D_{4h} symmetry of the starting product $Mn_2H_{10}^{10-}$ is broken, the leaving hydrogens are involved in four molecular orbitals. Two of them, $1a_1$ and $1b_2$ in Figure 2, are occupied metal–hydrogen bonding orbitals (**16** and **17**). The two others are unoccupied and are their metal–hydrogen antibonding counterparts $3a_1$ and $3b_2$ (**18** and **19**).[14] A simplified orbital

(13) Hoffmann, R. *Angew. Chem.* **1982**, *94*, 725; *Angew. Chem., Int. Ed. Engl.* **1982**, *21*, 711.

(14) Note however that at the very beginning of the reaction, the LUMO $3b_2$ is the metal–metal antibonding σ MO of $Mn_2H_{10}^{10-}$.

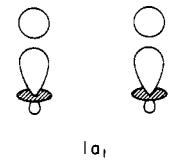

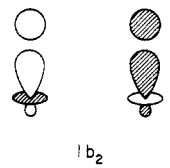

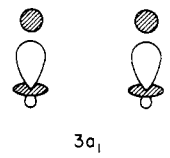

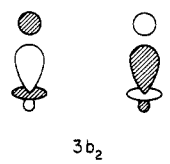

correspondence, without taking into account the avoided crossings, is given for this reaction in Figure 4a. In the course of the reaction, the $1a_1$ and $1b_2$ occupied orbitals, which have larger coefficients on the hydrogens, correlate with the σ and σ^* orbital, respectively, of the eliminated H_2. The $3a_1$ and $3b_2$ unoccupied orbitals, which have larger coefficients on the metals, correlate with the metal π and π^* orbitals, respectively, of the D_{2h} $Mn_2H_8^{10-}$ final product, i.e., the $b_{1u}(\pi_u)$ (**20**) and the $b_{2g}(\pi^*_g)$ (**21**) in Figure 3. The

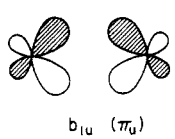

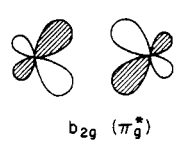

a_1 metal–metal σ-bonding orbital keeps its nature, although it is destabilized in the final product because the a_1 MO of ML_4 (**15**) is higher than the a_1 MO of ML_5 (**13**). The remaining MO's do not change a lot during the course of the reaction. Note that there is a MO of b_2 symmetry in the d block. Now, taking into account the necessary avoidance of orbitals of the same symmetry, the approximate correlations of Figure 4b take place. $1a_1$ correlates with $\sigma(H_2)$, $1b_2$ correlates with the b_2 of the d block, the $2b_2$ of the d block correlates with the unoccupied π^*, $2a_1$ correlates with the occupied π, $3a_1$ correlates with the metal–metal σ, and $3b_2$ correlates with $\sigma^*(H_2)$.

In reality other avoided crossings occur because there are other orbitals of a_1 and b_2 symmetry between the σ and σ^* orbitals of H_2. But the essence of the reaction is contained in this scheme. The real level crossing occurs between the $2b_2$ and $3a_1$. In Figure 2 it occurs at about 75% of the progress of the reaction, which is the location of the barrier calculated in Figure 1. Basically the same scheme is valid for the variant of the reaction **11** → **12** that has carbonyls as ligands. The MO correlation diagram in that

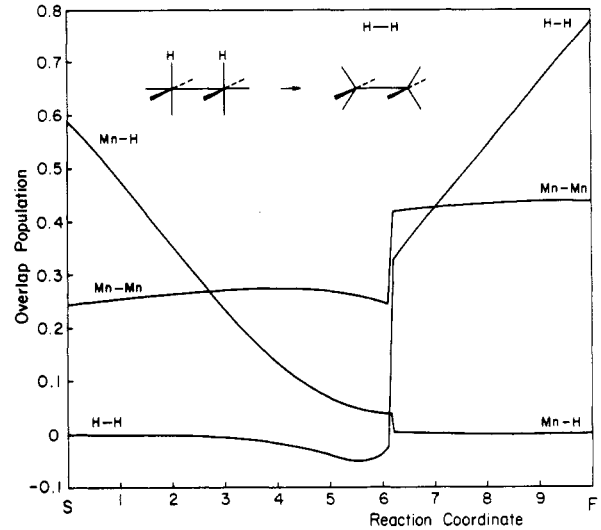

Figure 5. Evolution of the total overlap population for the bonds Mn–Mn, Mn–H, and H–H along the C_{2v} least-motion reductive elimination of H_2 from $Mn_2(CO)_8H_2^{2-}$.

case is made more complicated by additional ligand orbitals. These add avoided crossings, and furthermore metal orbitals are now mixed with carbonyl orbitals. The real crossing between the crucial a_1 and b_2 MO's takes place at about 60% of the advance along the reaction coordinate and the barrier occurs at that stage.

In Figure 5 we show the evolution of the total overlap population for the bonds that undergo a change in reaction **11** → **12**. The Mn–H bonds that are broken evolve fairly monotonically from 0.59 to 0. The Mn–Mn bond, which changes from single to double multiplicity, increases from 0.25 to 0.44. The H–H bond that is formed evolves from 0 to 0.78. For these two bonds, the variations are not monotonic and exhibit the characteristic discontinuities occurring at the level crossing.

The Organic Parallel. The dinuclear reductive elimination reaction is therefore clearly a forbidden reaction. To gain further understanding let us carry out a parallel comparison with the organic analogue of this reaction, namely, the concerted cis elimination from alkanes. This reaction is known to be symmetry forbidden in a least-motion pathway. We show in Figure 6 the calculated orbital correlation diagram for the C_{2v} least-motion cis elimination of H_2 from C_2H_6. The calculated energy profile along this reaction exhibits a barrier of 7.3 eV, while the final products are only 0.4 eV above the reactant. Let us detail what happens in this reaction. Once the D_{2h} symmetry of ethane is broken, at the very beginning of the reaction, the leaving hydrogen atoms are involved in four orbitals. Two of them, $1a_1$ and $1b_2$, are occupied and are the in-phase and out-of-phase combinations of the carbon–hydrogen bonding orbitals (**22**). The two other or-

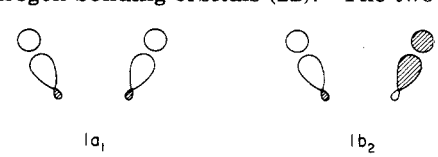

22

bitals, $2a_1$ and $2b_2$, which are empty, are their antibonding counterparts (**23**). The orbital correspondences along the reaction, without taking into consideration the avoided crossings, are represented in Figure 7a. $1a_1$ and $1b_2$ correlate with the σ and σ^* MO's of the leaving H_2. $2a_1$ and $2b_2$, which have larger coefficients on carbon, correlate with

23

the π and π^* of the formed ethylene. Taking into account the avoided crossings leads to the simplified correlation diagram drawn in Figure 7b.[15] A level crossing still persists between the frontier orbitals $1b_2$ and $2a_1$, which makes this reaction a forbidden reaction.

Now, can we forge a link between the organic and inorganic cases? In other words, is it possible to understand and predict Figure 4b from Figure 7b? The answer is straightforward. The correlations are very similar. In going from the organic reaction to the inorganic reaction, a d block of six occupied orbitals has been introduced. This set contains a b_2 orbital that interferes in the correlations only by adding an avoided crossing. Another difference between C_2H_4 and d^8 M_2L_8 is the ordering of the a_1 σ and π bonding orbitals. In d^8 M_2L_8 the σ metal–metal bonding orbital is above the π metal–metal bonding orbital. This is a direct consequence of the b_2, a_1 ordering for C_{2v} d^8 ML_4 (15), whereas isolobal methylene CH_2 has an a_1, b_2 ordering (24). However, these changes are minor and the crossing that makes the reaction 11 → 12 forbidden is basically the same one that occurs in the cis elimination from ethane.

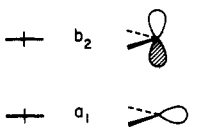

24

Trying To Evade the Forbiddeness of the Least-Motion Pathway. Can we modify the electron count on the metal to get rid of the level crossing? Since our $M_2L_8H_2$ reactant is a saturated 18-electron species, it would not be realistic to add two extra electrons to this species. Note, on Figure 4 that this could suppress the level crossing but would populate the π^* MO of M_2L_8 and eventually the σ^* MO on $M_2L_8H_2$, altering or destroying the metal–metal bonding. Removing one or several pairs of electrons would also destroy or weaken the metal–metal bonding in each species and incidentally would not prevent the reaction from being forbidden (see Figure 4b). Therefore, because of the metal–metal bond, we have no latitude to modify the electron count on the metal for these models. This contrasts with the mononuclear case where such a requirement was not present.[11b]

Let us modify now our model itself, using another isolobal analogy, 25. According to this isolobal analogy, the

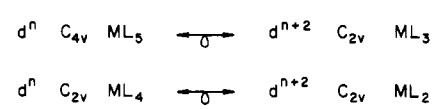

25

bonding in our models should not be modified if we remove the lateral (y direction) ligands in reaction 11 → 12 and add two more electrons on each metal. In effect, for either the reactant or the reduced product, the orbitals involved in the metal–metal bond are basically the same (26 and 27). The new model reaction is now that of 28. We chose

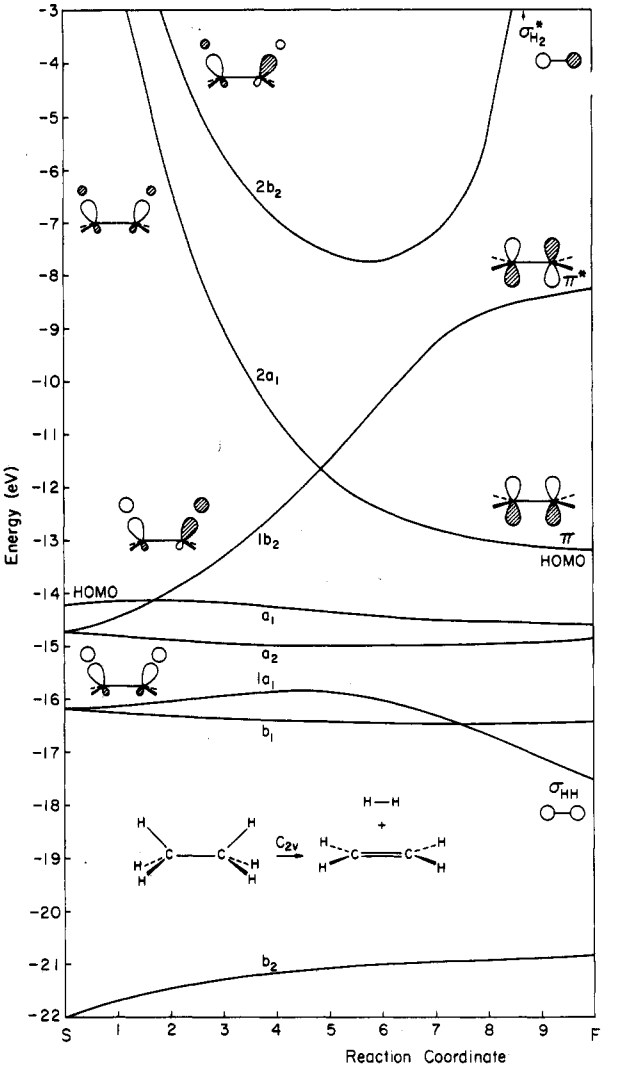

Figure 6. Orbital correlation diagram for the C_{2v} least-motion cis elimination of H_2 from C_2H_6.

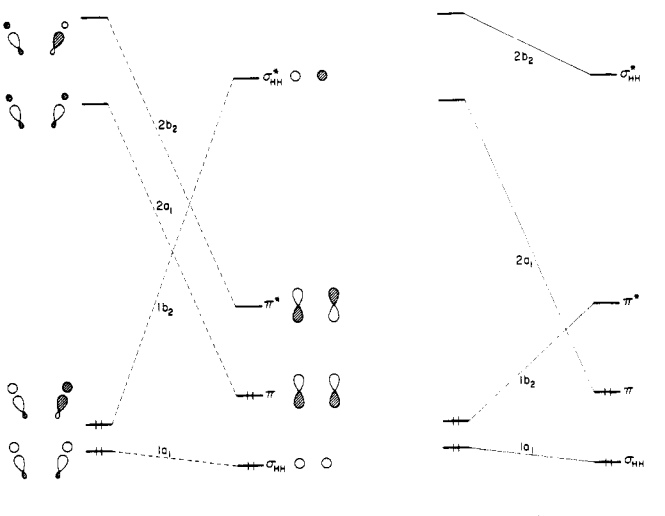

Figure 7. Schematic correlation diagram for the C_{2v} least-motion cis elimination of H_2 from C_2H_6: (a) before taking into account the avoided level crossings; (b) after taking into account the avoided level crossings.

(15) The a_1 MO corresponding to the σ C–C bond undergoes little change along the reaction, as can be seen in Figure 6. Since it does not interfere with the other levels, this MO has been omitted for clarity in Figure 7.

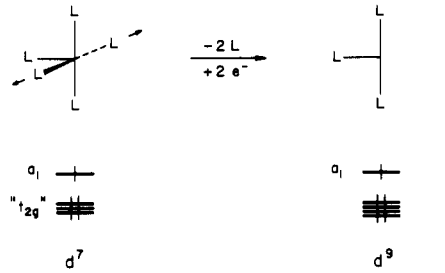

26

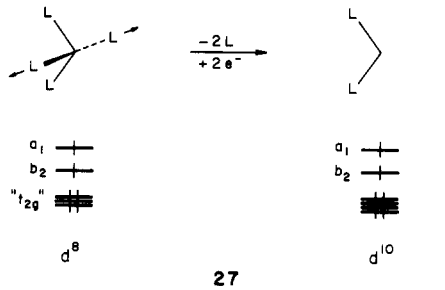

27

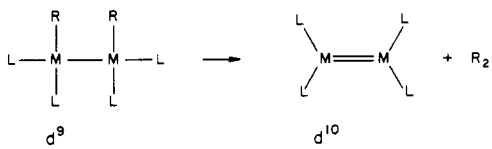

28

as a reactant 16-electron square-planar binuclear complex in **28** a model d^9 complex of cobalt(0): $Co_2H_6^{6-}$. We then calculated a C_{2v} least-motion pathway for the reaction shown in **29**. As expected, the correlation diagram for this reaction presents the same major characteristics as the one for reaction **11** → **12**. The reaction is forbidden. It has an energy barrier calculated at 6.3 eV, while the reaction energy is +3.4 eV.

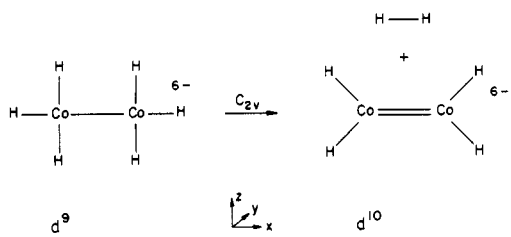

29

Dinuclear reductive eliminations from 16-electron square-planar complexes are therefore similar to reductive eliminations from 18-electron $M_2L_8R_2$ complexes and are forbidden for this C_{2v} least-motion pathway. At this point, it is interesting to point out that this differs from the mononuclear reaction. Cis reductive elimination from a 16-electron square-planar ML_2R_2 complex turns out to be allowed in a C_{2v} least-motion pathway.[11b]

Before trying to search for non-least-motion pathways, let us see if we can make easier the least-motion pathway, i.e., lower the energy barrier, by playing with the nature of the ligands. From the correlation diagrams in Figures 2 and 4b, the main level that could influence the height of the barrier is the a_1 HOMO level (σ metal–metal bond) of the final product. A lowering of this level should induce the crossing earlier in the reaction and reduce the energy barrier. The reverse effect can be expected from a raising of this level. From a simple perturbation viewpoint, this level should be lowered by electron acceptor substituents and raised by electron donor substituents (**30**).

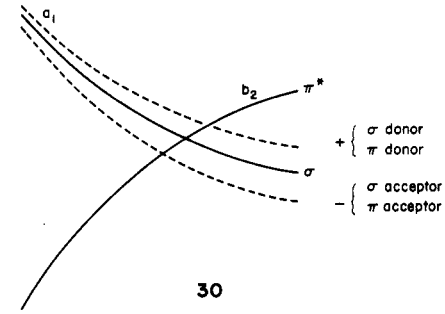

30

As far as σ effects are concerned, one can simulate easily acceptor or donor substituents by playing with the extended Hückel H_{ii} parameters for the spectator hydrogens in reaction **11** → **12**. We therefore computed again reaction **11** → **12** using first a 1s orbital energy (H_{ii}) for the spectator hydrogens, at −15.6 eV. This mimics σ acceptor ligands. Then we used a value of −11.75 eV that simulates σ donor ligands. The energetic changes induced by these substituent effects are in the expected directions, as in **30**, but are tiny. The crucial σ level is shifted by only ±0.2 eV; the activation barrier is modified only by about the same quantity. This small effect may come from the fact that this σ orbital has very small coefficients on the ligand.

π effects should operate in the same direction. Using carbonyls as ligands in reaction **11** → **12** supports this argument. The a_1 σ HOMO of the final product $(CO)_4Mn{=}Mn(CO)_4^{2-}$ is at −11.3 eV, which corresponds to a lowering of 2.5 eV with respect to $H_4Mn{=}MnH_4^{10-}$. This ensures an increased stability for the reaction product and therefore a reduced reaction energy and activation barrier. The high stabilization of this a_1 σ MO is due to the stabilization of the a_1 orbital in the C_{2v} ML_4 fragment (**15**). Replacement of hydrides by carbonyls in the C_{2v} ML_4 fragment lowers all the orbitals by π conjugation with the carbonyl π^* MO's. This effect is more pronounced for the a_1 orbital, which is now delocalized into the carbonyls (**31**).

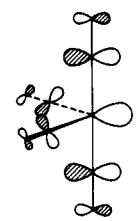

31

This a_1 orbital is therefore highly stabilized in energy, but since it is delocalized all over the molecule, the overlap for σ metal–metal bonding should be slightly reduced. The leading effect is by far the energy lowering, which in turn ensures a low a_1 σ metal–metal bonding orbital in the dinuclear species M_2L_4 when L is a π acceptor. Cyano groups, CN^-, which are π acceptors, too, should induce similar changes in the energy profile of the reaction.

Last, we have replaced the spectator ligands by typical π donor ligands, namely, Cl^-. In $Mn_2Cl_8^{10-}$ the metal orbitals have been pushed up, except for the HOMO a_1 σ which is now at −9.2 eV. The π^* LUMO has been pushed down; this results in a very narrow HOMO–LUMO gap. The calculated energy profile for the reaction $Mn_2Cl_8H_2^{10-}$ → $Mn_2Cl_8^{10-}$ + H_2 is a monotonic ascent up to +11.8 eV. Halogen ligands therefore make the reaction unfavorable in the direction of the reductive elimination. Accordingly it should be easy in the direction of the oxidative addition. This is not in contradiction with the facts observed for reaction **5**.

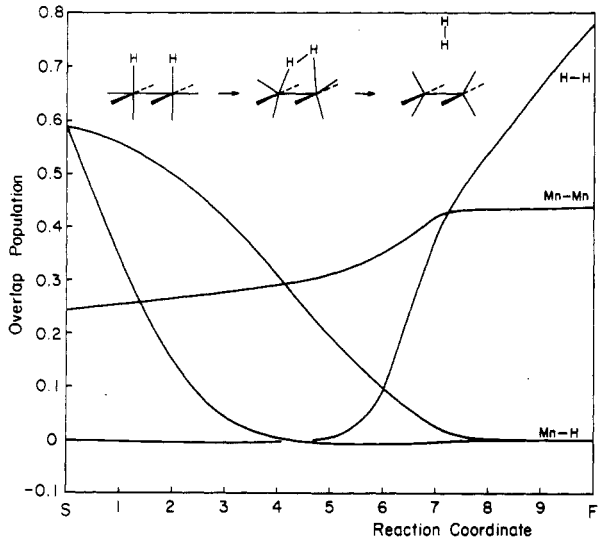

Figure 8. Evolution of the total overlap population for the bonds Mn–Mn, Mn–H, and H–H along the C_s reductive elimination of H_2 from $Mn_2(CO)_8H_2^{2-}$.

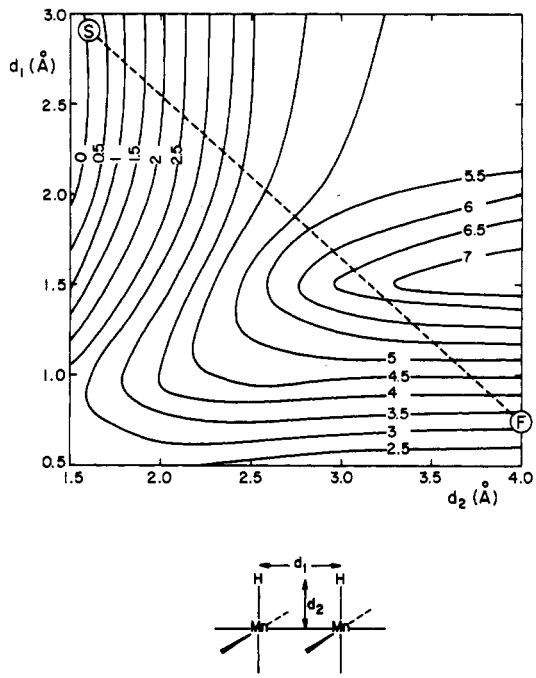

Figure 9. Potential energy surface for planar C_{2v} motions of the hydrogen atoms in $Mn_2(CO)_8H_2^{2-}$. The energy contours are in electronvolts relative to the starting idealized geometry *S*.

In conclusion, the substituent effects follow the expected scheme (**30**), and π effects are predominant over the σ ones. The magnitude of the reaction-facilitating effects achieved by realistic ligands is, however, not impressive.

Search for Non-Least-Motion Pathways. Since the level crossing for both organic (Figure 7b) and inorganic (Figure 4b) C_{2v} reactions occurs between orbitals of a_1 and b_2 symmetry, it should persist if the reaction is carried out under C_2 symmetry, as in **32**. In effect the corresponding

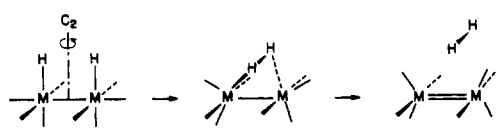

32

orbitals are now of a and b symmetry and still can cross

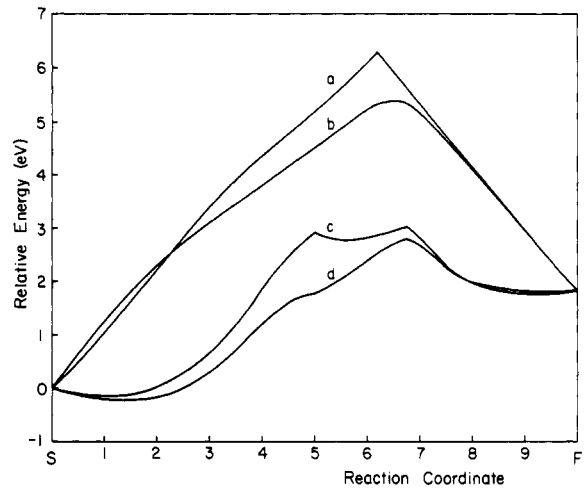

Figure 10. Summary of the energy profiles calculated for the reductive elimination of H_2 from $Mn_2(CO)_8H_2^{2-}$: (a) C_{2v} least-motion pathway; (b) C_s pathway; (c) C_{2v} two-step pathway with waypoint I; (d) C_{2v} two-step pathway with waypoint I′.

each other. This is no longer possible if the reaction is carried out under reduced C_s symmetry (**33**), M–M and

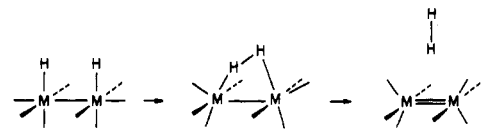

33

H–H bonds remaining in the same plane along the reaction. Now the two corresponding orbitals are both of a′ symmetry and cannot cross each other. The reaction thus becomes formally allowed. Such a pathway has been calculated for our model with carbonyls as ligands. Although an energy barrier still remains, it has been lowered by $\simeq$1 eV. The variations in total overlap population for the Mn–Mn, Mn–H, and H–H bonds are displayed in Figure 8. Note that there are now two types of Mn–H bonds during the reaction. The curves are now smooth and no longer exhibit the discontinuities characteristic of a real level crossing in Figure 5.

Let us see now if there could be other non-least-motion pathways that further lower the activation energy. In Figure 9, a two-dimensional potential surface is plotted for the C_{2v} movements of the leaving hydrogens in the *xz* plane (**34**) in $Mn_2(CO)_8H_2^{2-}$. Note that the positions of the

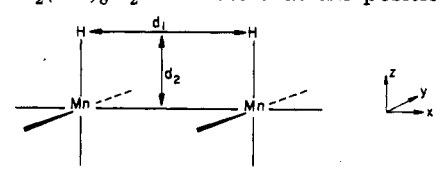

34

starting material S and the final product F do not correspond exactly to minima on the surface. This is not unexpected from the known problems of the extended Hückel model. The movement of the hydrogens during the C_{2v} least-motion pathway **11** → **12** corresponds to the straight line S–F in Figure 9. An easier pathway is suggested for a contraction of d_1, coupled with a slight shortening of d_2, followed by the full variation of d_2. This is nothing else than the C_{2v} bending of the Mn–H bonds (**35**) to form the H–H bond, followed by removal of the H_2

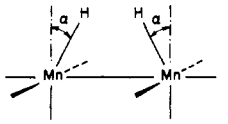

35

along the z direction. We therefore computed a C_{2v} two-step pathway (**36**) in which the first step consists of a

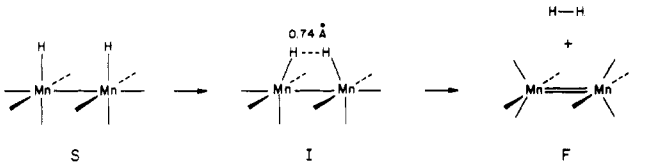

36

simple bending of the Mn–H bonds up to $\alpha = 42.45°$; this corresponds to a distance of 0.74 Å between the two hydrogens, which is already the final geometry for H_2. The energy profile for this reaction is given in curve C in Figure 10. The energy barrier has been considerably reduced with respect to the one-step C_{2v} least-motion pathway (curve a) or its modification to avoid the level crossing (curve b). In the initial step of the reaction, the energy first decreases, giving a minimum for $\alpha \simeq 10°$. The stabilization obtained in this bending motion is due to the formation of the hydrogen–hydrogen bond, while the metal–hydrogen bonds are still strong. The Walsh diagram for the reaction shows that the a_1 MO corresponding to the in-phase combination of the two M–H bonds is pushed down at the very beginning of the reaction, contrary to what occurred in the C_{2v} one-step reaction. After completion of the bending, in the waypoint I, the orbital corresponding to the σ H–H bond lies at −17.7 eV and is 78% on hydrogen, with a small remnant of metal d_σ components (**37**).

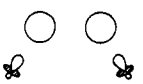

37

On the other hand, the b_2 MO corresponding to the out-of-plane combination of the two M–H bonds has been pushed up, but only moderately so, to −11.0 eV. Both factors contribute to put I only ≃3 eV above the starting product, which is half of the barrier occurring in the one-step least-motion pathway. This is also illustrated by the variation of the overlap populations shown in Figure 11. For the waypoint I, the overlap population between the two hydrogens is quite large, 0.47, while the overlap population between Mn and H still remains important, 0.33. More remarkable is that the H···H overlap population keeps a near zero value at the beginning of the bending, without becoming negative as in the C_{2v} one-step reaction (Figure 5).

At this point, one could question the validity of this positive overlap population between two hydrogens that still remain linked to the metal. To give us some more confidence that this is not an artifact due to our method, we carried out some further model calculations. First, a similar bending of the two CH bonds in ethane (**38**) was explored. The variation of overlap populations during this

38

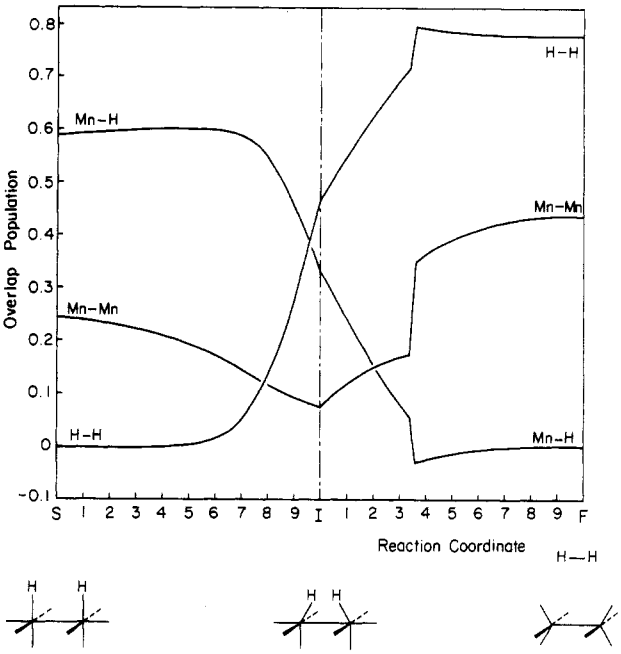

Figure 11. Evolution of the total overlap population for the bonds Mn–Mn, Mn–H and H–H along the C_{2v} two-step reductive elimination of H_2 from $Mn_2(CO)_8H_2^{2-}$.

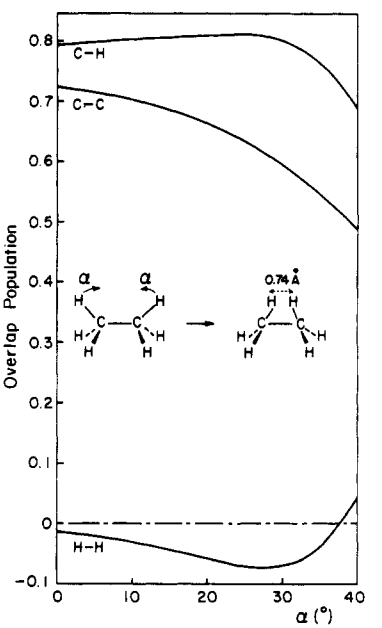

Figure 12. Evolution of the total overlap population for the bonds C–C, C–H, and H–H during the bending of two C–H bonds in ethane.

motion is reported in Figure 12. In this case, the H···H overlap population first becomes negative but eventually takes on a positive value at the end of the reaction. The variations of the C–H and C–C overlap populations are quite similawr to the Mn–H and Mn–Mn ones in the left part of Figure 11. The trends are therefore similar in the organic and inorganic cases.

We also studied an intermolecular model, in which two C–H bonds and two Mn–H bonds were brought together in a colinear way (**39** and **40**). It turns out that as the hydrogens are brought as near as d = 0.74 Å, the H–H overlap population (Figure 13) remains positive in both cases while the C–H and Mn–H overlap populations decrease but still maintain a substantial value. Here also, the hydrogens linked to the metal undergo greater changes than the hydrogen linked to the carbon.

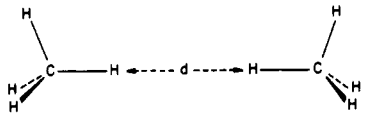

39

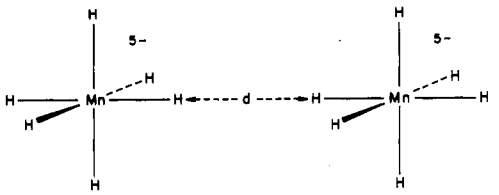

40

It is remarkable to find substantial H–H bonding between two hydrogens formally bound to other atoms. This is not what one would anticipate from simple chemical intuition, and one also knows that in real molecules steric hindrance between two C–H bonds that get in each other's way has structural and thermodynamic consequences. Our calculations also exhibit steric repulsion—the total energies rise steeply in reactions **39** and **40** as d decreases. But still there is a positive H···H overlap population, a sign of bonding.

Simple first-order interaction of filled C–H (or M–H) levels cannot lead to a positive H–H overlap population. The effect must be due to second-order mixing or to an interaction of σ levels in one component with σ^* levels in the other. We intend to explore this phenomenon in more detail. It is also necessary to check the essential observation of a positive overlap population with other computational methods, since the extended Hückel procedure does particularly badly for H_2.

Turning back to the second step of reaction **36**, the level crossing that occurs in this step does not induce an important energy barrier (Figure 10c, right). If this step is carried out under reduced C_s symmetry, the crossing is just avoided and does not change significantly the energy profile. However, it is legitimate to expect that the energy profile for the whole reaction can be smoothed by an adequate mixing of the two reaction coordinates that we have so far kept separate. A potential energy surface corresponding to the bending α of the two Mn–H bonds and the rocking β of the in-plane Mn–CO bonds in $Mn_2(CO)_8H_2^{2-}$ (**41**) led us to construct a new C_{2v} pathway with

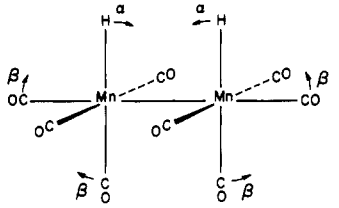

41

β coupled to α. This path has a waypoint I′ (**42**), in which

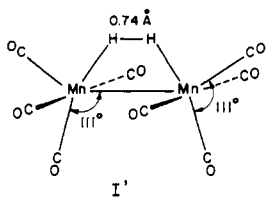

42

I′

the in-plane carbonyls were rotated to an optimal position. I′ is only 1.8 eV above the starting point. In the second step of the reaction, the energy rises up to 2.8 eV, but the

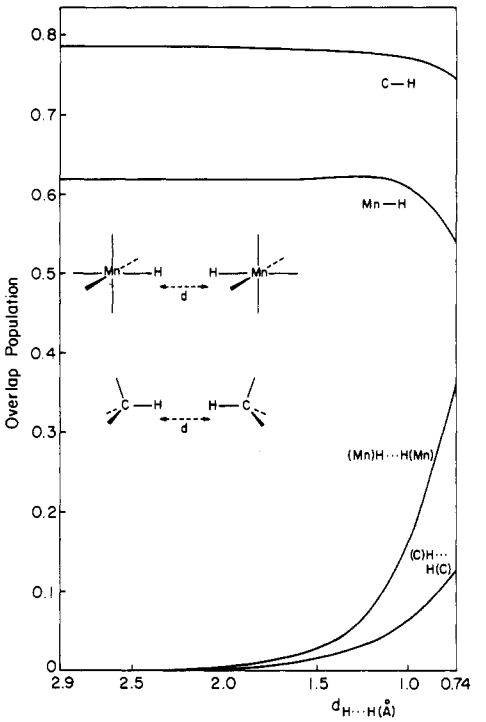

Figure 13. Evolution of the total overlap population for the bonds C–H and H–H during the colinear approach of two C–H bonds from two CH_4 and for the bonds Mn–H and H–H during the colinear approach of two Mn–H bonds from two MnH_6^{5-}.

energy profile for this pathway is now smoother. Here also, if the second step is carried out under reduced C_s symmetry, this does not lower the barrier. The new reaction profile is curve d in Figure 10, which summarizes the four energy profiles that were calculated for the reductive elimination of H_2 from $Mn_2(CO)_8H_2^{2-}$. Obviously, the lowest curve in Figure 10 could be further smoothed by considering other non-least-motion pathways, but we think this will not lower the energy barrier any further.

It is interesting to note that if we carry out the cis elimination of H_2 from C_2H_6 in a two-step pathway with initial bending of the CH bonds as in **38**, this does not lower significantly the activation energy with respect to the least-motion reaction. Here, the level crossing that occurs in the second step induces a barrier comparable to the one observed during the least-motion pathway.

Throughout this work, we have considered hydrogens as leaving groups. If we had taken alkyl groups, such as methyl, this would have increased the barriers for any of the reactions studied herein. In effect, even if each methyl group keeps a C_{3v} local symmetry during the reaction, a tilting angle θ of these C_3 axes has to be introduced in the course of the reactions (**43**), and no doubt this would cost some energy.

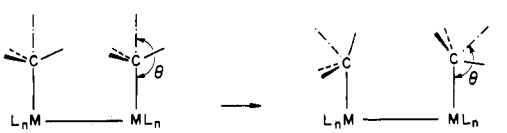

43

Even when we have reduced the barrier to dinuclear reductive elimination as much as possible, through the strategies described above, the reaction remains a kinetically and thermodynamically unfavorable one. This is because it is fundamentally a forbidden reaction, like its organic analogue, cis elimination from alkanes. We thus

Table I. Parameters Used in Extended Hückel Calculations

	orbital	H_{ii}, eV	ζ_1	ζ_2	C_1 [a]	C_2 [a]
Mn	4s	−9.75	1.80			
	4p	−5.89	1.80			
	3d	−11.67	5.15	1.70	0.5139	0.6929
Co	4s	−9.21	2.00			
	4p	−5.29	2.00			
	3d	−13.18	5.55	1.90	0.5551	0.6461
C	2s	−21.40	1.625			
	2p	−11.40	1.625			
O	2s	−32.30	2.275			
	2p	−14.80	2.275			
Cl	3s	−30.00	2.033			
	3p	−15.00	2.033			
H	1s	−13.60	1.30			

[a] Contraction coefficients used in the double-ζ expansion.

understand the infrequent occurrence of this type of reaction. There is a fundamental difference between mononuclear and dinuclear reductive elimination.

Incidentally, the reverse reaction to dinuclear elimination, dinuclear oxidative addition, is suggested to be thermodynamically more favorable, although still forbidden. Some possible examples of this reaction were discussed in the Introduction.

It is interesting to note that the concerted dinuclear reductive elimination is an allowed photochemical reaction, as Figure 4b shows. The required excitation should be mainly metal $\sigma \rightarrow \pi^*$ in character. A recent case of photochemical elimination of ethane from an A-frame dimethyl complex has been reported.[16]

Returning to the elimination reaction, one consequence of the unfavorable nature of the dinuclear elimination is that alternatives such as **44**, the analogue of a 2 + 2 + 2 symmetry-allowed reaction, might enter as reaction channels for binuclear complexes. Such a reaction for ML_n = $Os(CO)_4$, R = CH_3, is observed.[101]

44

The energy barrier to dinuclear elimination is significantly lowered when the leaving groups are first bent toward each other. If the leaving group were forced to anticipate this motion in the starting material, the elimination could occur more easily. This could be done by introducing sterically cumbersome ligands in a proper position (**45**) or by tying the leaving groups together (**46**).

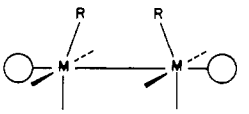

45

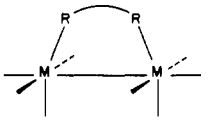

46

Acknowledgment. The permanent address of Georges Trinquier is the Laboratoire de Physique Quantique, Université Paul-Sabatier, Toulouse, France. His stay at Cornell was made possible by a NATO grant. We are grateful to the National Science Foundation for its support of this work through research grant, CHE 7828048. We thank Jane Jorgensen for the drawings and Eleanor Stolz for the typing.

Appendix

All calculations were performed by using the extended Hückel method[17] with weighted H_{ij}'s. Idealized geometries were assumed, and standard bond lengths and bond angles were used. $M_2L_8H_2$ was assumed to have an octahedral environment at each metal center. Planar $Co_2H_6^{6-}$ was assumed to have H–Co–H angles of 90°. For Mn_2L_8 a trigonal-bipyramid local environment was assumed at each metal center. The H–Co–H angles in $Co_2H_4^{6-}$ were fixed at 90° in order to obtain a MO ordering that allows us to fill two bonding MO's, in a doubly bonded picture. For the same reason the metal–metal bonds were optimized in Mn_2L_8 and $Co_2H_4^{6-}$. The H–C–H angles in C_2H_6 were fixed at 109.47°. The H–C–H angles in C_2H_4 were fixed at 120°. The following bond distances were used: Mn—H = 1.60 Å, Mn—Mn = 2.90 Å, Mn—C = 1.85 Å, C—O = 1.16 Å, Mn—Cl = 2.40 Å, Mn═Mn = 2.50 Å in $Mn_2(CO)_8^{2-}$ and 2.40 Å in $Mn_2H_8^{10-}$, Co—H = 1.60 Å, Co—Co = 2.50 Å, Co═Co = 2.00 Å, H—H = 0.74 Å, C—H = 1.09 Å, C—C = 1.54 Å, C═C = 1.34 Å.

The reaction coordinates consist of 10 synchronous regular variations of bond lengths, bond angles, and dihedral angles along the reactions. For the one-step reactions, the leaving hydrogens are defined by the H–H and HH–MM distances, denoted as d_1 and d_2, respectively, in **34**. For the C_s reaction, another parameter is introduced, namely, the rocking of H–H, that enables H—H and M═M to be perpendicular at the end of the reaction. The final point for the C_{2v} reductive elimination corresponds to a distance of 4.00 Å between H—H and M═M. The final point for the C_s reductive elimination corresponds to a distance of 4.00 Å between the lower hydrogen of H_2 and M═M. The final point for the cis elimination of H_2 from C_2H_6 corresponds to a distance of 3.00 Å between H—H and C═C.

The extended Hückel parameters used in our calculations are listed in Table I.

Registry No. 11 (L = H^-), 88288-62-4; 11 (L = CO), 88288-66-8; 12 (L = H^-), 88288-63-5; 12 (L = CO), 88288-67-9; $Mn_2Cl_8H_2^{10-}$, 88288-68-0; $Mn_2Cl_8^{10-}$, 88288-69-1; $Co_2H_6^{6-}$, 88288-64-6; $Co_2H_4^{6-}$, 88288-65-7; C_2H_6, 74-84-0.

(16) Hill, R. H.; Puddephatt, R. J. *Organometallics* **1983**, 2, 1472.

(17) Hoffmann, R. *J. Chem. Phys.* **1963**, *39*, 1397.